Lake Surface Temperature Dynamics as Precursors to Glacial Lake Outburst Floods: A Case Study of Lake Merzbacher, Central Tianshan

Meixia Wang[1,2], Donghui Shangguan[1,2,3*], Da Li[1], Yaojun Li[1], Rongjun Wang[1], Asim Qayyum Butt[1], Jinkui Wu[1]

[1] State Key Laboratory of Cryospheric Science and Frozen Soil Engineering/ Tanggula Mountain Cryosphere and Environment Observation and Research Station of Tibet Autonomous Region, Northwest Institute of Eco-Environment and Resources, Chinese Academy of Sciences, Lanzhou, 730000, China

[2] University of Chinese Academy of Sciences, Beijing, 101408, China

[3] China-Pakistan Joint Research Centre on Earth Sciences, CAS-HEC, Islamabad, 45320, Pakistan

Correspondence: Donghui Shangguan (dhguan@lzb.ac.cn).

Abstract

Glacial lake outburst floods (GLOFs) have become increasingly frequent under climate warming, yet the extent to which lake surface temperature (LST) can provide diagnostic information on ice-dammed lake outbursts remains insufficiently understood. This study investigates the potential of MODIS-derived LST as a remotely sensed precursor for GLOFs at Lake Merzbacher, Kyrgyzstan, one of the most frequently outbursting ice-dammed lakes in central Tianshan Mountain. We analyzed LST trends from 2000 to 2022 and examined short-term LST dynamics preceding 25 documented GLOF events. The results reveal a significant summer LST warming trend of 0.06 °C yr^{-1}, exceeding the regional air temperature increase. Approximately 90% of GLOFs occurred when LST exceeded 12 °C, indicating that this value can be used as an empirical, site-specific LST reference level for identifying the warm-season window of elevated outburst likelihood, rather than as a deterministic trigger threshold. Distinct short-term thermal signals were also detected before outburst, including a rapid LST increase peaking at 0.65 °C·d^{-1} around 8 days before drainage and an empirical acceleration signal exceeding 1.04 °C·d^{-2} around 9 days before outburst. This study shows that MODIS-derived LST can provide supplementary diagnostic information for ice-dammed lake monitoring. We propose a multi-parameter framework integrating

LST, LST anomalies, the rate of LST change, LST acceleration, lake area, lake level or volume estimates, and ice-dam response indicators to support early-warning systems. In addition, peak discharge showed the strongest correlation with 15-day cumulative LST before outburst ($r = 0.77$), suggesting that short-term surface thermal accumulation is statistically associated with flood magnitude. These results indicate that MODIS-derived LST can provide supplementary diagnostic information for ice-dammed lake monitoring. We propose a multi-parameter framework integrating LST, LST anomalies, LST change rate, LST acceleration, lake area, lake level or volume estimates, and ice-dam response indicators to support early-warning systems.

Keywords: Lake Merzbacher, GLOF, lake surface temperature, early warning, ice-dammed lake

1. Introduction

Glacial lake outburst floods (GLOFs) are increasingly recognized as a significant hazard in High Mountain Asia (HMA), where accelerated atmospheric warming has driven widespread glacier mass loss and rapid expansion of glacial lakes over recent decades (Hugonnet et al., 2021; Veh et al., 2023). In the Tianshan Mountains, where warming rates exceed 0.3°C per decade, glacier retreat has led to the formation and enlargement of numerous proglacial and ice-dammed lakes, elevating the risk of ice-dam failure and related floods (Wang et al., 2013; Chen et al., 2016). Ice-dammed lakes are particularly hazardous because they may drain suddenly and repeatedly, causing substantial economic damage and loss of life ((Carrivick and Tweed, 2016; Shangguan et al., 2017; Li et al., 2021). Although real-time monitoring systems have improved early warning capabilities (Zheng et al., 2021), predicting the timing of ice-dam failure remains difficult due to their complex and often inaccessible settings (Gu et al., 2023).

GLOF initiation can result from dynamic external disturbances such as rockfalls, ice avalanches, or rapid water input, as well as long-term processes that modify dam stability, including ice melt, permafrost degradation, and evolving subglacial hydrology (Richardson and Reynolds, 2000; Chikita and Yamada, 2005; Rounce et al., 2016). Among these drivers, air temperature has been widely linked to GLOFs through its control on glacier meltwater supply and internal ice-dam weakening (Ng et al., 2007; Ng and Liu, 2009). Yet, despite its acknowledged importance, the temperature sensitivity of ice-dammed lakes—and especially the direct response of lake surface

temperature (LST)—remains poorly quantified. The physical mechanism of GLOF initiation varies among lake types. Some glacial lakes drain by overtopping or overflow into supraglacial channels, whereas others may drain through mechanical dam instability or through the opening, connection, and enlargement of englacial or subglacial drainage pathways (Sattar et al., 2022; Remya et al., 2025). For ice-dammed lakes such as Lake Merzbacher, drainage is generally more closely linked to lake filling, increasing hydrostatic pressure, partial ice-dam flotation, and the development of englacial or subglacial conduits than to simple surface overflow or catastrophic dam collapse (Kingslake and Ng, 2013; Häusler et al., 2016).

Lake Merzbacher, located between the Northern and Southern Inylchek glaciers, represents one of the world's most frequently draining ice-dammed lakes, with documented GLOFs since 1931 (Mayr et al., 2014). Annual outbursts typically occur between June and October, coinciding with peak meltwater supply during warm summer conditions (Ng and Liu, 2009). Previous studies have developed remote-sensing-based indices to identify pre-outburst signals (Xie et al., 2013) and have quantified the predictability of the timing of dam failure (Kingslake and Ng, 2013). However, a key knowledge gap remains: the role of LST dynamics prior to GLOFs has not yet been systematically evaluated, despite LST being a potentially useful indicator of regional climate forcing, lake-surface thermal conditions, and open-water exposure (Austin and Colman, 2007; Zhang et al., 2014; Debnath et al., 2018; Attiah et al., 2023).

In this paper, we investigate whether fluctuations in lake surface temperature can provide diagnostic information about the timing and magnitude of GLOFs at Lake Merzbacher. Using MODIS-derived daily LST, we aim to:

(1) Characterize LST evolution in the days to weeks preceding GLOFs;

(2) Quantify LST change rates and accelerations as potential early-warning indicators;

(3) Evaluate the statistical association between short-term cumulative LST and peak flood discharge.

These analyses provide new insights into LST-based diagnostic indicators of ice-dammed lake outbursts and contribute to the development of multi-parameter monitoring tools for GLOF hazard assessment in remote alpine environments.

2. Study area

Lake Merzbacher is situated in the remote Inylchek region in the central Tianshan mountain range in Kyrgyzstan, bordering China, at the confluence of the Northern and

Southern Inylchek Glaciers at an altitude of about 3100 m, as illustrated in Figure 1. As described below, Northern Inylchek Glacier terminates in a proglacial lake, and down valley lies an ice-dammed lake (impounded by Southern Inylchek Glacier) that has repeatedly outburst to deliver glacier outburst floods (Häusler et al., 2016). Northern Inylchek Glacier and its neighbour Southern Inylchek Glacier comprise the largest compound glacier system in the central Tianshan Mountains. Although located in Kyrgyzstan, both glaciers drain into the Inylchek River. It feeds the Sary-Dshaz River in Kyrgyzstan, whose runoff flows into the Kumarik River of the main tributary of the Aksu River in China to feed that country's largest inland river, the Tarim, which provides a vital water supply to oases around the Taklamakan Desert (Mayr et al., 2014) (Fig. 1a). Glacial meltwater contributes at least 35% of the Tarim's total runoff (Aizen and Aizen, 1998). This proportion is predicted to rise over the next few decades (Aizen et al., 2007).

Lake Merzbacher is not a moraine-dammed lake but a repeatedly draining ice-dammed lake controlled by the interaction between lake filling and the Southern Inylchek ice dam (Glazirin, 2010). The lake typically fills during the warm season when glacier meltwater supply increases, and drainage occurs through englacial or subglacial pathways once the lake–ice-dam system reaches a critical hydromechanical state (Mayr et al., 2014). Previous studies have shown that the outburst process is closely related to changes in lake area, floating-ice coverage, ice-dam displacement, and the evolution of subglacial drainage (Ng et al., 2007; Mayr et al., 2014; Shangguan et al., 2017). In particular, high lake levels may promote partial flotation or uplift of the ice dam, allowing water to penetrate beneath or through the dam and initiate rapid drainage (Bolch, 2007). These characteristics make Lake Merzbacher an ideal site for testing whether remotely sensed LST can provide additional diagnostic information on the thermal preconditioning of GLOFs. In this study, LST is therefore interpreted in relation to seasonal meltwater supply, lake filling, open-water exposure, and possible thermal effects on drainage-channel enlargement, rather than as an independent trigger of ice-dam failure.

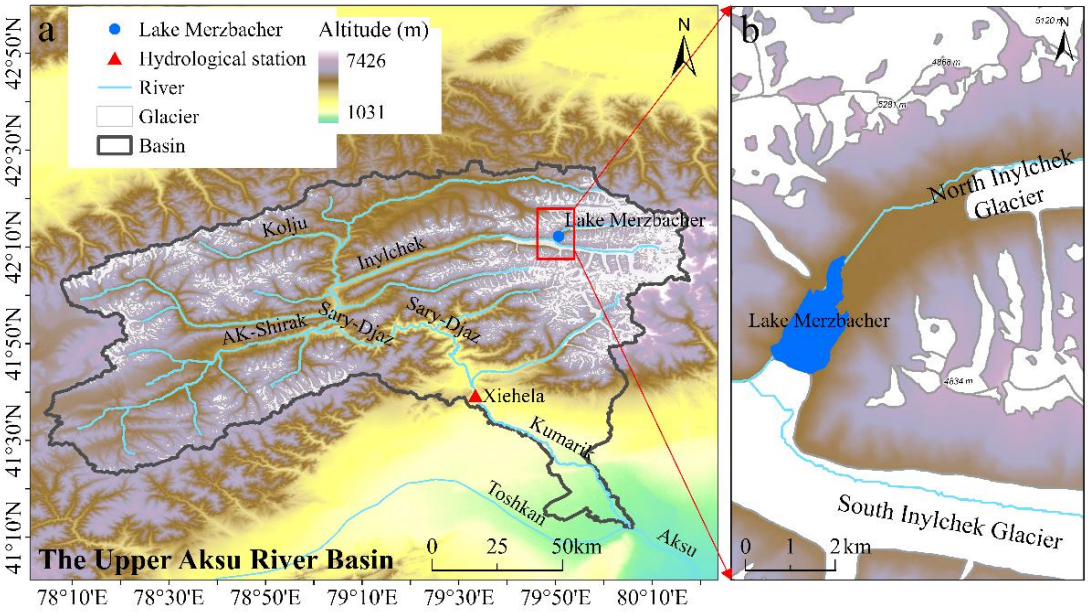

Figure 1. Location and glacio-hydrological setting of Lake Merzbacher in the central Tianshan Mountains. (a) Topography, glacier distribution, river network, basin boundary, Lake Merzbacher, and the Xiehela hydrological station in the Upper Aksu River Basin. (b) Enlarged map of Lake Merzbacher and the adjacent North Inylchek and South Inylchek glaciers. Land, glaciers, and water bodies are distinguished by different colours and are indicated in the legend.

3. Data and Methods

3.1 Glacial Lake Area and GLOF Records

The area of glacial lakes is a key predictor of susceptibility and hazard (Allen et al., 2019). For Lake Merzbacher, historical lake area from 1990 to 2015 and documented outburst dates from 2000 to 2015 were obtained from published sources (Liu, 1993; Glazirin, 2010; Kingslake and Ng, 2013; Shangguan et al., 2017; Li et al., 2020). Lake area and outburst dates from 2016 to 2022 were extracted from high-resolution Planet Scope (DOVA) satellite imagery (Table S1, Supplementary Material). Planet's Dove satellites are CubeSats that weigh 4 kilograms (1000 times lower than other commercial imaging satellites), 10 by 10 by 30 centimetres in length, width and height, orbit at a height of about 400 kilometres and provide imagery with a resolution of 3-5 metres and are envisaged for environmental, humanitarian, and business applications.

For each documented GLOF, the pre-outburst lake area was obtained from the available satellite imagery. A total of 25 GLOF events from 2000 to 2022 were included in this study. Since 2000, no GLOF events triggered by glacier surges were reported in Lake Merzbacher (Liu et al., 2023).

3.2 Lake Surface Temperature Data

Lake surface temperature (LST) was derived from the MODIS Terra Land Surface Temperature Daily L3 Global 1 km product (MOD11A1). In this study, LST was derived from the daytime MODIS LST product; therefore, the values represent daytime radiometric lake surface skin temperature rather than daily mean bulk water temperature. MODIS LST has been shown to accurately reflect in situ lake temperature measurements at Lake Merzbacher, with $R^2 = 0.79$ for 2009–2010 observations (Bormudoi et al., 2012).

To address missing data, gap-filling was performed using the Climate Forecast System Version 2 (CFSv2)–MODIS integration in Google Earth Engine, generating continuous 1 km LST time series (Shiff et al., 2021). The filled dataset (CFSv2_LST) was evaluated against the original MODIS LST using mean absolute error (MAE), bias, and R^2, yielding high consistency ($R^2 = 0.95$, MAE = 1.31°C; Figure S1).

3.3 LST Temporal Analysis

In meteorology, a moving average is commonly used with time series data to smooth out short-term fluctuations and highlight longer-term trends for mean daily air temperatures (Hewitson and Crane, 1996). For the filled daily lake surface temperature (LST) series, the five-day moving average was used to produce smooth LST curves. Xie et al. (2013) divided Lake Merzbacher into four periods according to the outburst index: icefall, quick water storage, early-warning and post-drainage. During these four periods, the lake is filled with water and the water movement is slow; it takes about one month for an outburst to occur and about a week for the lake to empty after the drainage (Xie et al., 2013). Therefore, in this paper, the first and second derivative of the daily LST were calculated for one month before and one week after the glacial lake outburst.

The 25 documented GLOF events were aligned according to their outburst dates, with day 0 representing the GLOF date, negative values indicating days before the outburst, and positive values indicating days after the outburst. For each event, the first and second derivatives of the smoothed daily LST series were calculated over the window from 30 days before to 7 days after the outburst. The first derivative, dLST/dt, was used to describe the rate of LST change, with units of $°C \cdot d^{-1}$. The second derivative, d^2LST/dt^2, was used to describe the acceleration of LST change, with units of $°C \cdot d^{-2}$.

To identify significantly accelerated warming, all event-aligned d^2LST/dt^2 values from the 25 GLOF event windows were pooled. The mean μ and standard deviation σ

of these d^2LST/dt^2 values were then calculated, where μ denotes the mean LST acceleration and σ denotes its standard deviation. The acceleration threshold was defined as $\mu + 1.5\sigma$. Values of d^2LST/dt^2 exceeding this threshold were classified as significantly accelerated warming periods. For each GLOF event, the frequency of such accelerated warming periods was then counted within the 30 days before outburst.

To characterize short-term surface thermal accumulation before each outburst, we calculated a positive cumulative LST index over different pre-outburst windows. This index was defined as the sum of positive daily MODIS-derived LST values before the GLOF event and was used as an empirical indicator of surface thermal conditions and open-water exposure. It should not be interpreted as a direct estimate of lake-water heat content, subaqueous melt, or ice-dam ablation, because MODIS LST represents only the radiometric surface skin temperature of the lake (Austin and Colman, 2007; Zhang et al., 2014). The surface temperature may differ from the temperature at depth, at the lake bottom, or at the ice–water interface, especially under vertical thermal stratification (Attiah et al., 2023) (Figure. 2).

The positive cumulative LST index was calculated as:

$$T_A^{(N)} = \sum_{k=1}^{N} \max(T_k, 0)$$

where $T_A^{(N)}$ denotes the cumulative positive LST during the N days before the outburst, T_k is the corrected daily mean MODIS-derived LST on day k before the outburst, and N is the length of the accumulation window. Only positive LST values were accumulated; days with LST ≤ 0 °C were assigned a value of zero in the cumulative index. It should be noted that MODIS-derived LST does not directly represent the thermal conditions at depth or at the ice–water interface. For water temperatures below approximately 4 °C, density-driven stratification may allow near-surface water to remain close to 0 °C while deeper water is warmer (Cogley et al., 2011). Conversely, a positive surface temperature does not necessarily imply that the entire lake column is warm or that substantial subaqueous melt is occurring at the ice dam. Therefore, the cumulative LST index used here should be interpreted as a surface thermal precursor and an indicator of open-water thermal conditions, rather than as a direct measure of melt energy or ice-dam ablation (Liu et al., 2014). Direct lake-temperature profiles, lake-level observations, and ice-dam measurements would be required to quantify the relationship between surface thermal conditions and melt or drainage processes at depth.

In this study, to characterize trends in regional terrestrial air temperature, 2 m air temperatures (T) were obtained from the European Centre for Medium-Range Weather Forecasts (ECMWF) for the land component of the fifth-generation European Reanalysis dataset (ERA5-Land) for the period 2000–2022 (Muñoz-Sabater et al., 2021). Reanalysis data provide a consistent and globally complete description of past climate, allowing evaluation of regional warming trends relevant to LST dynamics and GLOF occurrence.

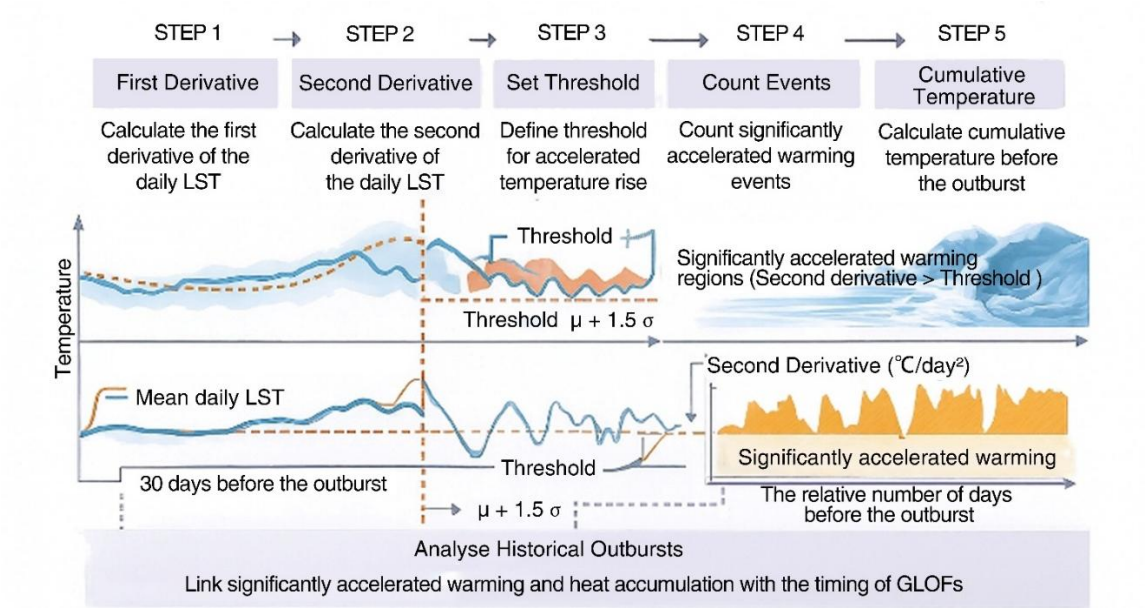

Figure 2. Schematic workflow for detecting thermal precursor signals before glacial lake outburst floods (GLOFs). The five steps shown at the top indicate the data-processing workflow. Daily MODIS-derived LST is first smoothed and differentiated to calculate the rate of LST change and its acceleration. The x-axis in the time-series panels represents days relative to the outburst date, with negative values indicating days before the GLOF. The blue line denotes the mean or smoothed daily LST, the light-blue shading indicates the variability among historical events, the orange dashed vertical line marks the outburst date, and the orange shaded areas indicate significantly accelerated warming periods where the second derivative exceeds the threshold μ + 1.5σ. These thermal indicators are then combined with cumulative LST before the outburst to evaluate their relationship with GLOF timing and magnitude.

4. Results

4.1 Temporal trends of LST, lake area, and GLOF timing

Temperature-anomaly analysis shows that MODIS-derived LST exhibited a stronger warming tendency than ERA5-Land 2 m air temperature during the core melt season, especially in July and August (Fig. 3). The July LST anomaly showed the largest positive trend, whereas trends in monthly T2m anomalies were weaker. Because

MODIS-derived LST represents daytime radiometric lake surface skin temperature and ERA5-Land T2m represents near-surface air temperature, these two variables should be compared in terms of anomalies and trends rather than absolute values.

Satellite image analysis from 1990 to 2022 revealed a declining trend in the maximum observed lake area (Fig. S2a). The average lake area over this period was 3.22 km², with a maximum of 3.95 km² on 9 August 1996 and a minimum of 2.12 km² on 4 July 2021. Because direct lake-volume observations are not available for all events, lake area is used here only as a first-order geometric proxy for lake storage. The timing of GLOFs advanced by approximately 0.6 days yr^{-1} (Fig. S2b), with most post-2000 events occurring from early July to mid-August. This earlier occurrence may be associated with changes in meltwater supply, lake filling rate, ice-dam geometry, and the evolving efficiency of englacial or subglacial drainage pathways.

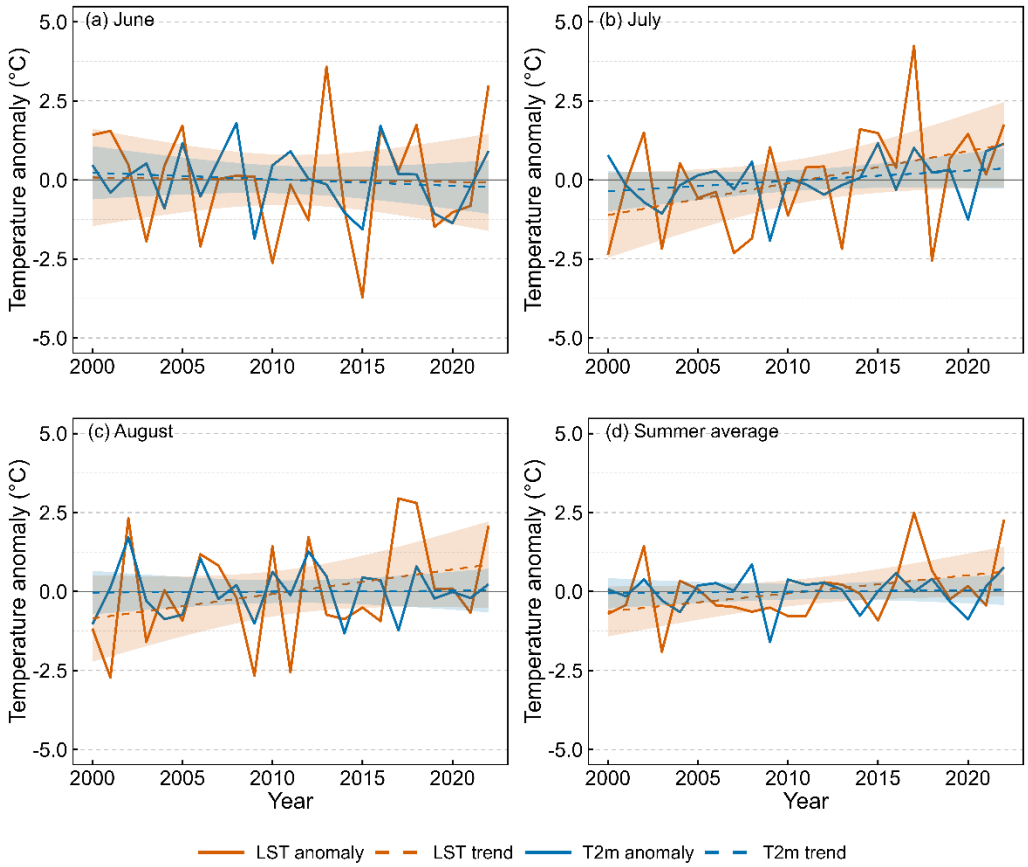

Figure 3. Interannual variations in monthly and summer temperature anomalies of MODIS-derived lake surface temperature (LST) and ERA5-Land 2 m air temperature (T2m) from 2000 to 2022. Temperature anomalies were calculated relative to the 2000–2022 mean for each month or season. Panels show June (a), July (b), August (c), and the June–August summer mean (d). Monthly values were calculated as the arithmetic

mean of all valid daily values within the corresponding month, and the summer mean was calculated as the average of June, July, and August monthly anomalies. Solid lines show annual anomalies, dashed lines show linear trends, and shaded areas indicate the 95 % confidence intervals of the trends.

4.2 Short-Term LST Dynamics Before the Glacial Lake Outburst

Analysis of LST in the 30-day window preceding each GLOF event reveals characteristic warming patterns. GLOFs predominantly occurred on days when LST exceeded 12 °C, with approximately 90 % of events falling within the 12–20 °C range (Fig. 4). The lake may remain stable at LST values above 12 °C if lake level, hydrostatic pressure, ice-dam flotation conditions, and englacial or subglacial drainage connectivity have not yet reached a critical state. For Lake Merzbacher, outburst initiation is more appropriately interpreted as the activation, connection, or enlargement of englacial and subglacial drainage pathways, probably associated with lake filling, increasing hydrostatic pressure, and partial ice-dam flotation (Kingslake and Ng, 2013). A few events occurred under very high LST conditions, exceeding 20 °C, for example 25.4 °C on 8 July 2017 and 23.5 °C on 10 August 2018, which may indicate periods of enhanced surface heating, meltwater input, and favorable conditions for drainage-system development (Chikita et al., 2000; Ogier et al., 2021). Therefore, the 12 °C level is used here as a non-deterministic thermal indicator of elevated outburst likelihood and should be combined with LST change rate, LST acceleration, lake filling, floating-ice coverage, water level, and ice-dam motion for early-warning purposes.

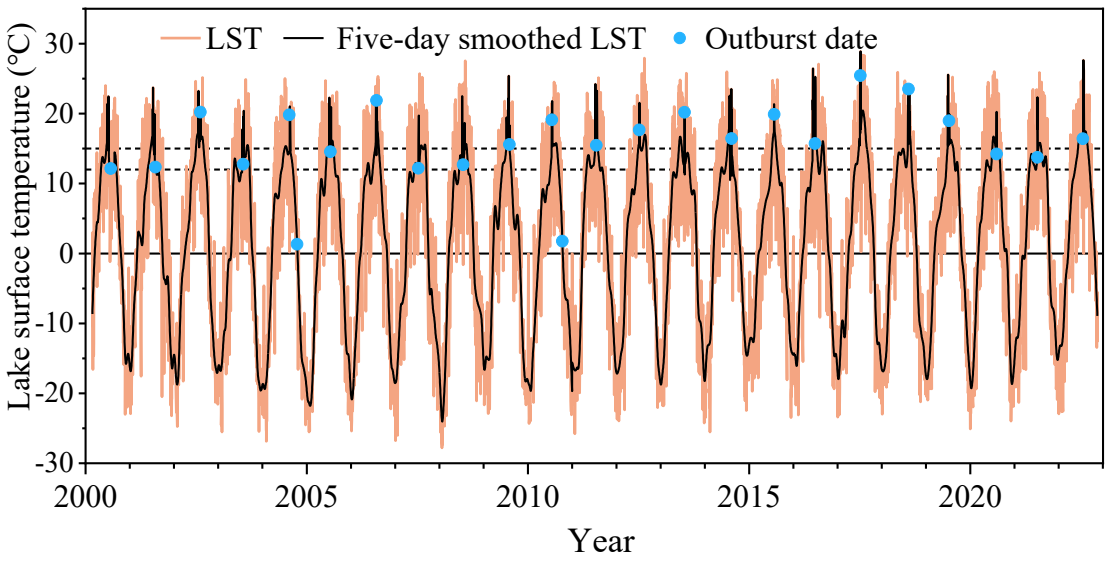

Figure 4. Lake surface temperature fluctuations in Lake Merzbacher from 2000 to 2022. Blue dot represents the outburst date of the glacial lake.

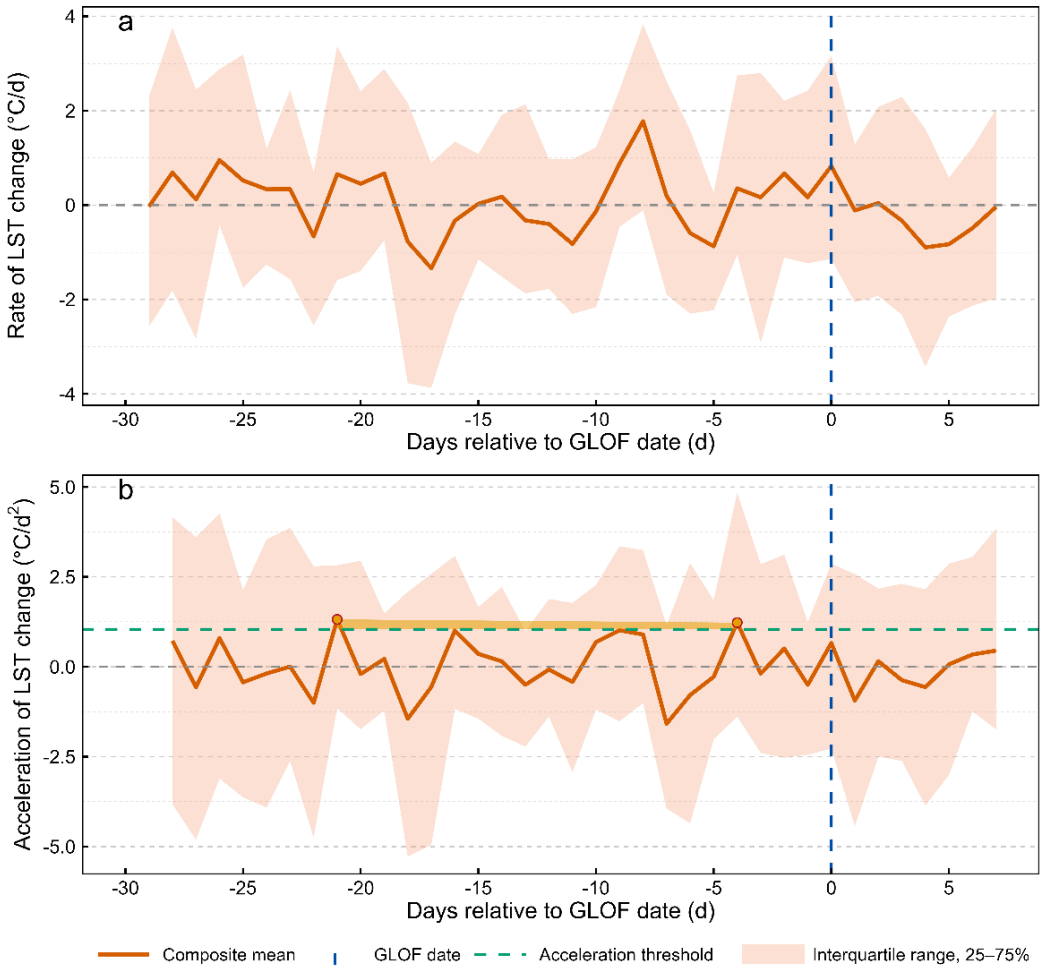

289

290 **Figure 5.** Composite short-term LST dynamics before and after GLOF events at Lake
291 Merzbacher. The curves were calculated by aligning the 25 documented GLOF events
292 to their outburst dates. Day 0 indicates the GLOF date, negative values indicate days
293 before the outburst, and positive values indicate days after the outburst. (a) Rate of LST
294 change, dLST/dt, in °C d^{-1}. (b) Acceleration of LST change, d^2LST/dt^2, in °C d^{-2}. The
295 thick orange-red line represents the multi-event composite mean, and the light-orange
296 envelope represents the interquartile range, 25–75 %. The vertical blue dashed line
297 marks the GLOF date, and the horizontal green dashed line in panel (b) indicates the
298 acceleration threshold of 1.04 °C d^{-2}.

299 Statistical analysis shows a rapid LST increase within approximately eight days
300 before outbursts (Fig. 5a). A two-sample t-test confirms the presence of a short-term
301 warming signal prior to GLOFs ($p < 0.05$). On the outburst day, the rate of LST change
302 peaks at 0.65 °C·day^{-1}.

303 To quantify thermal acceleration, the second derivative of LST was computed over a
304 30-day window centered on each outburst. Based on 25 historical events (Table S1), an

empirical acceleration threshold of 1.04 °C d^{-2} was identified for detecting unusually rapid LST increases in the event-aligned composite series. Two exceedances were observed: 22 days before the outburst (1.20 °C·day^{-2}) and 9 days before the outburst (1.16 °C·day^{-2}). The earlier signal may indicate the onset of accelerated thermal activity, while the latter corresponds to a pre-outburst thermal reinforcement phase, potentially defining a short-term diagnostic window for enhanced monitoring. Post-outburst, LST change rates decline rapidly and occasionally turn negative, reflecting system re-equilibration and meltwater inflow (Fig. 5b).

4.3 Short-Term Cumulative Temperature and Peak Discharge

Before interpreting the relationship between cumulative LST and peak discharge, it is important to note that flood magnitude is expected to be controlled at first order by the amount of water available for drainage. In the absence of direct lake-volume measurements for all events, the observed lake area provides only a first-order geometric proxy for lake storage. Therefore, cumulative LST is interpreted here as a supplementary surface thermal indicator that may modulate drainage efficiency, rather than as a replacement for lake-volume or lake-level controls.

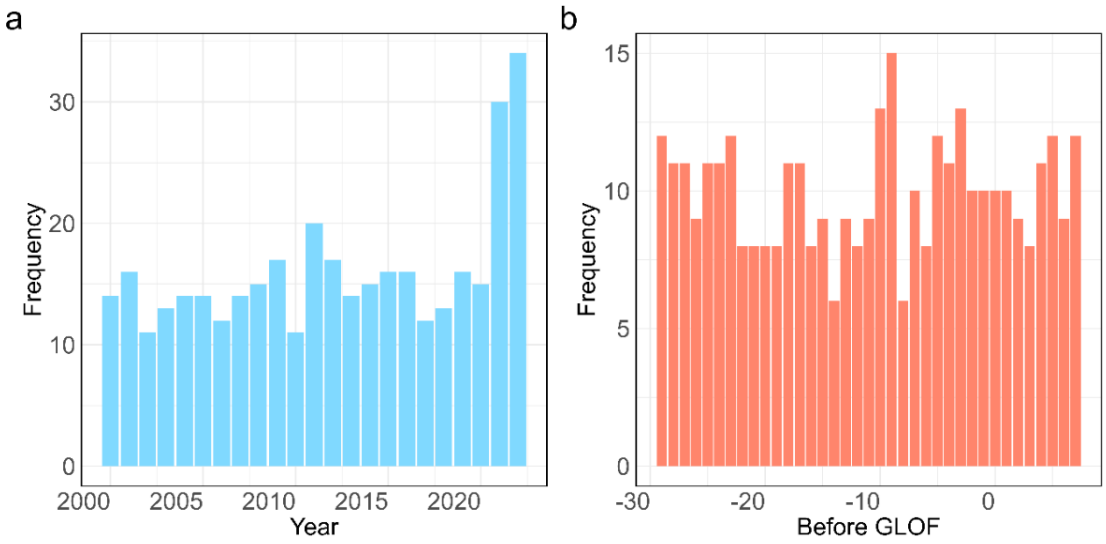

Figure 6. Frequency and timing of accelerated LST warming occurrences. An accelerated LST warming occurrence is defined as a daily value of d^2LST/dt^2 exceeding the empirical acceleration threshold of 1.04 °C d^{-2} within the event-aligned GLOF windows. (a) Annual frequency of accelerated LST warming occurrences from 2000 to 2022. (b) Distribution of accelerated LST warming occurrences by days relative to the GLOF date, where day 0 indicates the outburst date and negative values indicate days before outburst.

The frequency of accelerated LST warming occurrences increased in recent years,

particularly over the past decade, and reached its maximum in 2022 (Fig. 6a). Here, an accelerated LST warming occurrence is defined as a daily value within the event-aligned GLOF windows for which the LST acceleration, d^2LST/dt^2, exceeds the empirical threshold of 1.04 °C·d^{-2}. Therefore, these occurrences represent threshold-exceeding LST acceleration days, rather than independent GLOF events. From 2000 to the mid-2010s, such occurrences were relatively evenly distributed. Their timing relative to outburst dates shows a clear clustering approximately 10 days before GLOFs (Fig. 6b), suggesting that abrupt LST acceleration may provide a short-term diagnostic signal during the pre-outburst phase. Although threshold-exceeding acceleration occurs throughout the 30-day pre-outburst window, the localized peak indicates a period during which enhanced monitoring may be particularly useful.

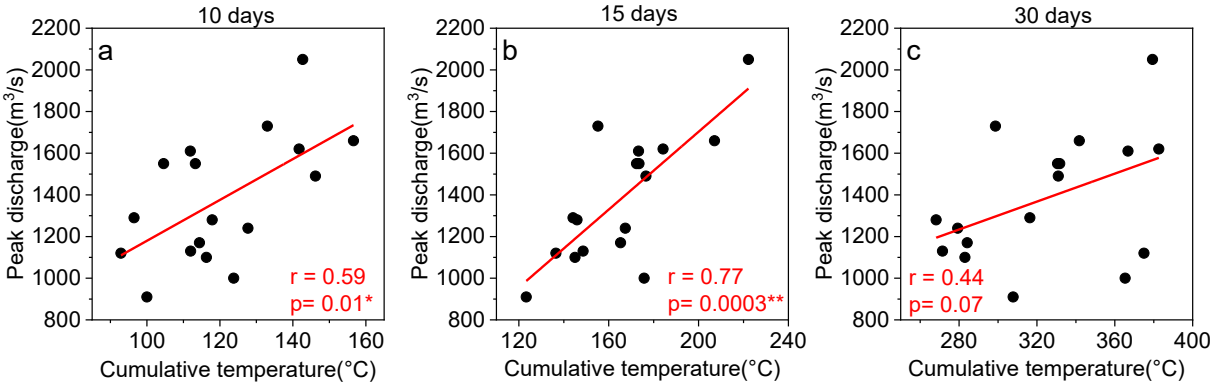

Figure 7. Relationships between short-term cumulative temperature and GLOF peak discharge. Correlation coefficients (r) and significance levels (p) are indicated for 10-, 15-, and 30-day accumulation windows.

To investigate whether short-term surface thermal conditions are associated with flood magnitude, we analyzed the relationships between GLOF peak discharge and cumulative LST over 10-day, 15-day, and 30-day windows before each outburst event (Fig. 7). Peak discharge is expected to be controlled at first order by the amount of water available for drainage, lake level, hydraulic head, drainage-pathway geometry, and the rate of enlargement of englacial or subglacial channels. Because direct lake-volume observations were not available for all events, lake area was used only as a first-order geometric proxy for lake storage. Cumulative LST should therefore be interpreted as a supplementary surface thermal index that may reflect conditions favorable for meltwater input, lake filling, and thermally enhanced drainage-channel enlargement.

A positive relationship was observed between cumulative LST and peak discharge for the shorter accumulation periods. For the 10-day accumulation window, higher

cumulative LST was associated with larger peak discharge ($r = 0.59$, $p = 0.01$). The relationship was strongest for the 15-day window ($r = 0.77$, $p = 0.0003$), suggesting that the 15-day cumulative LST index provides the strongest statistical association with peak discharge among the tested accumulation windows. In contrast, the 30-day cumulative LST showed a weaker and statistically insignificant relationship with peak discharge ($r = 0.44$, $p = 0.07$), indicating that longer accumulation windows may dilute the short-term surface thermal signal associated with the pre-outburst drainage state. Overall, these results suggest that cumulative LST is statistically associated with GLOF peak discharge, but the physical interpretation must be considered together with lake storage, lake level, ice-dam geometry, and englacial or subglacial drainage development.

5. Discussion

5.1 Mechanistic links and limits of LST as a GLOF precursor

This study identifies statistically consistent LST signals before GLOFs at Lake Merzbacher, including an empirical 12 °C LST reference level, a rapid warming phase several days before outburst, and a statistical association between 10–15-day cumulative LST and peak discharge. Therefore, the observed pre-outburst increase and acceleration in LST should be interpreted as remotely sensed precursor signals, indicating that the lake–ice-dam system is approaching a high-risk pre-drainage state. These signals likely reflect the combined effects of enhanced glacier meltwater supply, rapid lake filling, increased hydrostatic pressure, partial ice-dam flotation, and the connection or enlargement of englacial and subglacial drainage pathways (Ogier et al., 2021). As the lake level rises, water pressure at the ice-dam interface may approach the ice overburden pressure, promoting partial flotation or uplift of the ice dam and allowing water to penetrate beneath or through the dam (Mayr et al., 2014). In this hydrostatic-pressure-induced flotation and drainage-initiation mechanism, lake level, lake volume, ice-dam thickness, dam geometry, drainage-pathway connectivity, and heat transfer to conduit walls are the primary controls on drainage initiation (Ng et al., 2007; Ogier et al., 2021).

Within this framework, LST is more appropriately regarded as a process-related precursor rather than a standalone causal trigger. Elevated LST may reflect enhanced summer energy input, reduced floating-ice cover, increased open-water exposure, and intensified glacier meltwater supply to the lake. These conditions favor rapid lake filling and may bring the lake closer to the hydrostatic conditions required for flotation-induced drainage (Kingslake and Ng, 2013). Therefore, the observed pre-outburst LST

increase is likely linked to the preconditioning phase of GLOFs through its association with meltwater production, lake storage, and the seasonal evolution of the lake–ice-dam system (Emmer et al., 2022).

LST may also influence the drainage-evolution phase after drainage has initiated . Relatively warm lake water can enhance thermal erosion along englacial or subglacial conduits, thereby accelerating conduit enlargement and affecting the rising limb and magnitude of the outburst hydrograph (Austin and Colman, 2007). This interpretation is consistent with the observed positive correlation between short-term cumulative LST and peak discharge. Nevertheless, the present dataset does not allow us to distinguish whether thermal erosion initiates drainage or mainly amplifies discharge after a hydrostatic-pressure threshold has been reached. Direct observations of lake level, lake-water temperature profiles, ice-dam thickness, ice-dam displacement, and subglacial drainage evolution would be required to resolve this distinction.

5.2 Implications for early-warning system design

The LST indicators proposed in this study are most useful when incorporated into a multi-parameter early-warning framework rather than used as independent predictors. The 12 °C LST reference level may be used as a first-level empirical indicator of the warm-season window during which outbursts are more likely, but it should not be interpreted as a deterministic trigger threshold. Rapid LST increase and positive LST acceleration may provide short-term diagnostic information on the approach of a pre-drainage state. However, because Lake Merzbacher outbursts are likely controlled by hydrostatic pressure and ice-dam flotation, LST should be combined with variables that directly describe lake filling and dam response (Jenson et al., 2022).

A practical early-warning framework should therefore integrate: (1) absolute LST and LST anomalies, indicating lake thermal state; (2) $dLST/dt$ and d^2LST/dt^2, indicating rapid pre-outburst thermal change; (3) lake area and floating-ice coverage, indicating water storage and lake-surface evolution; (4) lake level or water-volume estimates, indicating hydrostatic pressure against the ice dam; (5) ice-dam displacement or surface velocity from GNSS, InSAR, or optical feature tracking, indicating possible flotation or mechanical adjustment of the dam; and (6) downstream discharge, seismic, or acoustic signals, indicating the onset of drainage. In such a framework, LST contributes valuable remotely sensed information, especially in remote alpine environments where in situ observations are limited, but it should be interpreted together with hydrological and glaciological indicators.

5.3 Non-stationarity of the LST indicator and future system evolution

The 12 °C LST reference level identified in this study is empirical, site-specific, and period-specific. The Lake Merzbacher system is non-static: glacier thinning, ice-dam lowering, changes in lake-basin geometry, variations in maximum lake volume, and evolving subglacial drainage efficiency may all modify the lake level required for flotation-induced drainage (Shangguan et al., 2017). As a result, the LST value associated with outburst occurrence may change over time even if the underlying hydrostatic mechanism remains similar.

The observed decline in maximum lake area and the advance in GLOF timing suggest that the lake–ice-dam system is already evolving (Li et al., 2020). Under continued climate warming, earlier snow and ice melt may shorten the lake-filling period and shift outbursts to earlier in summer (Veh et al., 2025). At the same time, glacier thinning and changes in dam geometry may reduce the storage volume required to initiate drainage or alter the hydraulic efficiency of subglacial conduits (Häusler et al., 2016). These changes could affect both the timing and magnitude of future GLOFs. Therefore, the LST threshold and acceleration criteria proposed here should be recalibrated regularly as new outburst events and updated satellite observations become available.

Overall, our results indicate that LST provides a useful remotely sensed precursor for Lake Merzbacher GLOFs, but its physical interpretation must be embedded within the broader lake-filling, ice-dam flotation, and subglacial drainage framework. Future work should combine thermal remote sensing with lake-level reconstruction, floating-ice monitoring, ice-dam displacement measurements, and coupled thermal–hydrological–mechanical modelling to better separate the roles of hydrostatic pressure and thermal erosion in the outburst process.

6. Conclusions

This study demonstrates that MODIS-derived lake surface temperature (LST) provides useful remotely sensed diagnostic information associated with the timing and magnitude of GLOFs at Lake Merzbacher. The main findings are as follows.

First, summer LST showed a warming trend of 0.06 °C yr^{-1} during 2000–2022, indicating that the lake surface is sensitive to warm-season thermal conditions. Second, approximately 90 % of documented GLOFs occurred when LST exceeded 12 °C. This value should be interpreted as an empirical, site-specific LST reference level marking the warm-season window of elevated outburst likelihood, rather than as a deterministic trigger threshold. Third, event-aligned analysis revealed short-term LST signals before

outburst, including a rapid warming phase of up to 0.65 °C·d^{-1} and an empirical acceleration signal exceeding 1.04 °C·d^{-2} around 9 days before drainage. Fourth, 10–15-day cumulative LST was statistically associated with peak discharge, with the strongest correlation found for the 15-day accumulation window.

These results suggest that LST can serve as a supplementary precursor within a multi-parameter early-warning framework. However, LST should not be interpreted as a standalone trigger or primary control of Lake Merzbacher outbursts. Drainage initiation is more likely governed by lake filling, lake level, hydrostatic pressure, ice-dam geometry, partial flotation, and the activation or enlargement of englacial and subglacial drainage pathways. Therefore, future monitoring should combine LST, LST change rate, LST acceleration, lake area, lake level or volume estimates, floating-ice coverage, ice-dam displacement, and downstream hydrological or seismic observations. The empirical LST reference level and acceleration criteria proposed here should be recalibrated as new GLOF events and updated satellite observations become available.

Data availability

The MODIS MOD11A1 LST product used in this study is available from the NASA Land Processes Distributed Active Archive Center (LP DAAC) at https://lpdaac.usgs.gov/data. ERA5-Land data are available from the European Centre for Medium-Range Weather Forecasts (ECMWF) at https://www.ecmwf.int/en/era5-land. Meteorological data are available from the China Meteorological Data Service Centre at http://data.cma.cn/en. Basic geographic data, including rivers, glaciers, and DEM data, were obtained from the National Tibetan Plateau Data Centre at https://data.tpdc.ac.cn. The processed data used in this study are available from the corresponding author upon reasonable request.

Financial support

This work was financially supported by the Key Research and Development Project of the Ministry of Science and Technology (grant no. 2025YFE0211400), the International Partnership of the Chinese Academy of Sciences (grant no. 046GJHZ2023069MI), the National Natural Science Foundation of China (grant nos. 42371145 and 42001068), the Gansu Province Postdoctoral Funding Project at the Northwest Institute of Eco-Environment and Resources (grant no. E539880320), the Gansu Provincial Natural Science Foundation (grant no. 25JRRA502), the Scientific

Research Project of Shule River Basin Water Resources Utilization Center, Gansu Province (grant no. SLH/KYXM-2025-01), and the Gansu Province Water Science Experimental Research and Technology Promotion Project (grant no. 25GSLK077).

Author contributions

Donghui Shangguan initiated the idea. Meixia Wang, Donghui Shangguan, and Da Li conceived the study. Meixia Wang and Da Li collected and processed the data. Meixia Wang performed the analysis, drafted the original manuscript, and designed the figures. Donghui Shangguan, Da Li, Yaojun Li, Rongjun Wang, and Jinkui Wu discussed the results. Asim Qayyum Butt polished the manuscript. All authors reviewed the manuscript and approved the final version.

Competing interests

The authors declare that they have no conflict of interest.

Copyright statement

References

Aizen, V. B. and Aizen, E. M.: Estimation of glacial runoff to the Tarim River, central Tien Shan, IAHS Publ., 248, 191–198, 1998.

Aizen, V. B., Aizen, E. M., and Kuzmichonok, V. A.: Glaciers and hydrological changes in the Tien Shan: simulation and prediction, Environ. Res. Lett., 2, 045019, https://doi.org/10.1088/1748-9326/2/4/045019, 2007.

Allen, S. K., Zhang, G., Wang, W., Yao, T., and Bolch, T.: Potentially dangerous glacial lakes across the Tibetan Plateau revealed using a large-scale automated assessment approach, Sci. Bull., 64, 435–445, https://doi.org/10.1016/j.scib.2019.03.011, 2019.

Attiah, G., Kheyrollah Pour, H., and Scott, K. A.: Lake surface temperature retrieved from Landsat satellite series (1984 to 2021) for the North Slave Region, Earth Syst. Sci. Data, 15, 1329–1355, https://doi.org/10.5194/essd-15-1329-2023, 2023.

Austin, J. A. and Colman, S. M.: Lake Superior summer water temperatures are increasing more rapidly than regional air temperatures: A positive ice-albedo feedback, Geophys. Res. Lett., 34, L06604, https://doi.org/10.1029/2006GL029021, 2007.

527 Bolch, T.: Climate change and glacier retreat in northern Tien Shan
528 (Kazakhstan/Kyrgyzstan) using remote sensing data, Global Planet. Change, 56, 1–
529 12, https://doi.org/10.1016/j.gloplacha.2006.07.009, 2007.
530 Bormudoi, A., Shabunin, A., Hazarika, M. K., Zaginaev, V., and Samarakoon, L.:
531 Studying the outburst of the Merzbacher lake of Inylchek Glacier, Kyrgyzstan with
532 remote sensing and field data, in: Proceedings of the 33rd Asian Conference on
533 Remote Sensing, Pattaya, Thailand, 2012.
534 Carrivick, J. L. and Tweed, F. S.: A global assessment of the societal impacts of glacier
535 outburst floods, Global Planet. Change, 144, 1–16,
536 https://doi.org/10.1016/j.gloplacha.2016.07.001, 2016.
537 Chen, Y., Li, W., Deng, H., Fang, G., and Li, Z.: Changes in Central Asia's Water Tower:
538 Past, Present and Future, Sci. Rep., 6, 39364, https://doi.org/10.1038/srep39364,
539 2016.
540 Chikita, K., Joshi, S. P., Jha, J., and Hasegawa, H.: Hydrological and thermal regimes
541 in a supra-glacial lake: Imja, Khumbu, Nepal Himalaya, Hydrol. Sci. J., 45, 507–521,
542 https://doi.org/10.1080/02626660009492353, 2000.
543 Debnath, M., Syiemlieh, H. J., Sharma, M. C., Kumar, R., Chowdhury, A., and Lal, U.:
544 Glacial lake dynamics and lake surface temperature assessment along the
545 Kangchengayo-Pauhunri Massif, Sikkim Himalaya, 1988–2014, Remote Sens. Appl.:
546 Soc. Environ., 9, 26–41, https://doi.org/10.1016/j.rsase.2017.11.002, 2018.
547 Emmer, A., Allen, S. K., Carey, M., Frey, H., Huggel, C., Korup, O., Mergili, M., Sattar,
548 A., Veh, G., Chen, T. Y., Cook, S. J., Correas-Gonzalez, M., Das, S., Diaz Moreno,
549 A., Drenkhan, F., Fischer, M., Immerzeel, W. W., Izagirre, E., Joshi, R. C.,
550 Kougkoulos, I., Kuyakanon Knapp, R., Li, D., Majeed, U., Matti, S., Moulton, H.,
551 Nick, F., Piroton, V., Rashid, I., Reza, M., Ribeiro De Figueiredo, A., Riveros, C.,
552 Shrestha, F., Shrestha, M., Steiner, J., Walker-Crawford, N., Wood, J. L., and Yde, J.
553 C.: Progress and challenges in glacial lake outburst flood research (2017–2021): a
554 research community perspective, Nat. Hazards Earth Syst. Sci., 22, 3041–3061,
555 https://doi.org/10.5194/nhess-22-3041-2022, 2022.
556 Glazirin, G. E.: A century of investigations on outbursts of the ice-dammed lake
557 Merzbacher (central Tien Shan), Austrian J. Earth Sci., 103, 171–179, 2010.
558 Gu, C., Li, S., Liu, M., Hu, K., and Wang, P.: Monitoring Glacier Lake Outburst Flood
559 (GLOF) of Lake Merzbacher Using Dense Chinese High-Resolution Satellite Images,
560 Remote Sens., 15, 1941, https://doi.org/10.3390/rs15071941, 2023.

Häusler, H., Ng, F., Kopecny, A., and Leber, D.: Remote-sensing-based analysis of the 1996 surge of Northern Inylchek Glacier, central Tien Shan, Kyrgyzstan, Geomorphology, 273, 292–307, https://doi.org/10.1016/j.geomorph.2016.08.021, 2016.

Hewitson, B. C. and Crane, R. G.: Climate downscaling: techniques and application, Clim. Res., 7, 85–95, https://doi.org/10.3354/cr007085, 1996.

Hugonnet, R., McNabb, R., Berthier, E., Menounos, B., Nuth, C., Girod, L., Farinotti, D., Huss, M., Dussaillant, I., Brun, F., and Kääb, A.: Accelerated global glacier mass loss in the early twenty-first century, Nature, 592, 726–731, https://doi.org/10.1038/s41586-021-03436-z, 2021.

Jenson, A., Amundson, J. M., Kingslake, J., and Hood, E.: Long-period variability in ice-dammed glacier outburst floods due to evolving catchment geometry, The Cryosphere, 16, 333–347, https://doi.org/10.5194/tc-16-333-2022, 2022.

Kingslake, J. and Ng, F.: Quantifying the predictability of the timing of jökulhlaups from Merzbacher Lake, Kyrgyzstan, J. Glaciol., 59, 805–818, https://doi.org/10.3189/2013JoG12J156, 2013.

Li, D., Shangguan, D., and Huang, W.: Research on the area change of Lake Merzbacher in the Tianshan Mountains during 1998–2017, J. Glaciol. Geocryol., 42, 1126–1134, https://doi.org/10.7522/j.issn.1000-0240.2019.0308, 2020.

Li, D., Shangguan, D., Wang, X., Ding, Y., Su, P., Liu, R., and Wang, M.: Expansion and hazard risk assessment of glacial lake Jialong Co in the central Himalayas by using an unmanned surface vessel and remote sensing, Sci. Total Environ., 784, 147249, https://doi.org/10.1016/j.scitotenv.2021.147249, 2021.

Liu, J.: Forecasting on Jokulhlaups in Kunmalike River, and its influence on river water condition, Southern Tianshan Mts, Hydrology, 25–30, https://doi.org/10.19797/j.cnki.1000-0852.1993.01.006, 1993.

Liu, J., Cheng, Z., and Su, P.: The relationship between air temperature fluctuation and Glacial Lake Outburst Floods in Tibet, China, Quatern. Int., 321, 78–87, https://doi.org/10.1016/j.quaint.2013.11.023, 2014.

Liu, J., Li, Z., and Liu, Y.: Glacier dammed lake outburst flood in cold season in the Tien Shan, China and Kyrgyzstan, Preprints [preprint], https://doi.org/10.20944/preprints202310.1666.v1, 2023.

Mayr, E., Juen, M., Mayer, C., Usubaliev, R., and Hagg, W.: Modeling Runoff from the Inylchek glaciers and Filling of Ice-Dammed Lake Merzbacher, Central Tian Shan,

595 Geogr. Ann. A, 96, 609–625, https://doi.org/10.1111/geoa.12061, 2014.
596 Muñoz-Sabater, J., Dutra, E., Agustí-Panareda, A., Albergel, C., Arduini, G., Balsamo,
597 G., Boussetta, S., Choulga, M., Harrigan, S., Hersbach, H., Martens, B., Miralles, D.
598 G., Piles, M., Rodríguez-Fernández, N. J., Zsoter, E., Buontempo, C., and Thépaut,
599 J.-N.: ERA5-Land: a state-of-the-art global reanalysis dataset for land applications,
600 Earth Syst. Sci. Data, 13, 4349–4383, https://doi.org/10.5194/essd-13-4349-2021,
601 2021.
602 Ng, F. and Liu, S.: Temporal dynamics of a jökulhlaup system, J. Glaciol., 55, 651–665,
603 https://doi.org/10.3189/002214309789470897, 2009.
604 Ng, F., Liu, S., Mavlyudov, B., and Wang, Y.: Climatic control on the peak discharge of
605 glacier outburst floods, Geophys. Res. Lett., 34, L21503,
606 https://doi.org/10.1029/2007GL031426, 2007.
607 Ogier, C., Werder, M. A., Huss, M., Kull, I., Hodel, D., and Farinotti, D.: Drainage of
608 an ice-dammed lake through a supraglacial stream: hydraulics and thermodynamics,
609 The Cryosphere, 15, 5133–5150, https://doi.org/10.5194/tc-15-5133-2021, 2021.
610 Remya, S. N., Nandan, V., Bhattacharya, A., Srinivasalu, P., Mukherjee, K., Govindha
611 Raj, B., Yackel, J., and Bolch, T.: Glacier calving and moraine collapse triggered the
612 glacial lake outburst flood in South Lhonak Lake, Indian Himalaya, Environ. Res.
613 Commun., 7, 115026, https://doi.org/10.1088/2515-7620/ae1936, 2025.
614 Richardson, S. D. and Reynolds, J. M.: An overview of glacial hazards in the Himalayas,
615 Quatern. Int., 65–66, 31–47, https://doi.org/10.1016/S1040-6182(99)00035-X, 2000.
616 Rounce, D. R., McKinney, D. C., Lala, J. M., Byers, A. C., and Watson, C. S.: A new
617 remote hazard and risk assessment framework for glacial lakes in the Nepal
618 Himalaya, Hydrol. Earth Syst. Sci., 20, 3455–3475, https://doi.org/10.5194/hess-20-
619 3455-2016, 2016.
620 Sattar, A., Haritashya, U. K., Kargel, J. S., and Karki, A.: Transition of a small
621 Himalayan glacier lake outburst flood to a giant transborder flood and debris flow,
622 Sci. Rep., 12, 12421, https://doi.org/10.1038/s41598-022-16337-6, 2022.
623 Shangguan, D., Ding, Y., Liu, S., Xie, Z., Pieczonka, T., Xu, J., and Moldobekov, B.:
624 Quick release of internal water storage in a glacier leads to underestimation of the
625 hazard potential of glacial lake outburst floods from Lake Merzbacher in central Tian
626 Shan Mountains: The risk of GLOF in Central Asia, Geophys. Res. Lett., 44, 9786–
627 9795, https://doi.org/10.1002/2017GL074443, 2017.
628 Shiff, S., Helman, D., and Lensky, I. M.: Worldwide continuous gap-filled MODIS land

surface temperature dataset, Sci. Data, 8, 74, https://doi.org/10.1038/s41597-021-00861-7, 2021.

Veh, G., Lützow, N., Tamm, J., Luna, L. V., Hugonnet, R., Vogel, K., Geertsema, M., Clague, J. J., and Korup, O.: Less extreme and earlier outbursts of ice-dammed lakes since 1900, Nature, 614, 701–707, https://doi.org/10.1038/s41586-022-05642-9, 2023.

Veh, G., Wang, B., Zirzow, A., Schmidt, C., Lützow, N., Steppat, F., Zhang, G., Vogel, K., Geertsema, M., Clague, J., and Korup, O.: Progressively smaller glacier lake outburst floods despite worldwide growth in lake area, Nat. Water, 3, 271–283, https://doi.org/10.1038/s44221-025-00388-w, 2025.

Wang, X., Wu, K., Jiang, L., Liu, S., Ding, Y., Jiang, Z., and Guo, W.: Wide expansion of glacial lakes in Tianshan Mountains during 1990–2010, Acta Geogr. Sin., 68, 983–993, 2013.

Xie, Z., Shangguan, D., Zhang, S., Ding, Y., and Liu, S.: Index for hazard of Glacier Lake Outburst flood of Lake Merzbacher by satellite-based monitoring of lake area and ice cover, Global Planet. Change, 107, 229–237, https://doi.org/10.1016/j.gloplacha.2012.05.025, 2013.

Zhang, G., Yao, T., Xie, H., Qin, J., Ye, Q., Dai, Y., and Guo, R.: Estimating surface temperature changes of lakes in the Tibetan Plateau using MODIS LST data, J. Geophys. Res.-Atmos., 119, 8552–8567, https://doi.org/10.1002/2014JD021615, 2014.

Zheng, G., Allen, S. K., Bao, A., Ballesteros-Cánovas, J. A., Huss, M., Zhang, G., Li, J., Yuan, Y., Jiang, L., Yu, T., Chen, W., and Stoffel, M.: Increasing risk of glacial lake outburst floods from future Third Pole deglaciation, Nat. Clim. Change, 11, 411–417, https://doi.org/10.1038/s41558-021-01028-3, 2021.